June 28, 2016

BACHELOR ASSIGNMENT

SYNTHESIS OF LINI$_{0.5}$MN$_{1.5}$O$_4$ NANOFIBERS BY ELECTROSPINNING

Martijn Mulder

Faculty of Science and Technology (TNW)
Inorganic Materials Science (IMS)

Exam committee:

Chairperson	prof.dr.ir. André ten Elshof
Daily Supervisor	ing. Karin van den Nieuwenhuijzen
External member	prof.dr.ir. Gertjan Koster
Member	ir. Gerard Cadafalch Gazquez

UNIVERSITY OF TWENTE

Abstract

This thesis explores a novel way of producing $LiNi_{0.5}Mn_{1.5}O_4$ nanofibers using the electrospinning method. This material is a candidate material for a new high-rate cathode for use in Lithium-ion batteries. Firstly the theoretical background was explored. Then a recipe to produce $LiNi_{0.5}Mn_{1.5}O_4$ by the sol-gel method was adapted to be able to produce the electrospun nanofibers. Furthermore different annealing processes have been proposed to anneal the $LiNi_{0.5}Mn_{1.5}O_4$ nanofibers without damaging the morphology. The morphology of the resulting samples was investigated using Scanning Electron Microscopy. The composition of the annealed material was determined by X-ray Diffraction. With this method it was found that it was possible to produce $LiNi_{0.5}Mn_{1.5}O_4$ nanofibers using the proposed recipe. However, it was found that the annealing process needs improvement, because thick samples are not annealed properly. Also, the XRD spectra showed that there was a second phase, probably consisting of $LiOH \cdot H_2O$ and Li_2O. Still a lot of work has to be done before electrospun $LiNi_{0.5}Mn_{1.5}O_4$ cathodes can be used in Lithium-ion batteries.

Acknowledgements

I would like to thank my supervisors for their support throughout the assignment. Firstly André for the regular progress meetings in which I could discuss all that I had done up to that point. This really helped me to keep going and stay motivated. Also I would like to thank him for being a listening ear whenever I had a question with which I struggled. Furthermore I would like to thank Karin for her practical help in the lab. I would not even have gotten this far, could I not have relied on her knowledge of the lab and its resources. Also Gerard deserves my thanks, for he dropped by to help whenever I had troubles with the microwave oven. Furthermore, my thanks to Gertjan for joining my exam committee on such short notice. I would also like to thank Moritz for being a great help whenever I did not understand the electrospinning setup and had questions about my results. The help we could give each other really contributed to making progress in the assignment. I would like to thank everyone in the Inorganic Materials Science (IMS) group for the many nice coffee breaks and colloquia that reset my mind so I could afterwards could start on my assignment fresh again. Lastly I would like to thank my friends and family for all the support they gave during my whole Bachelor and especially during this assignment.

Contents

Symbols & Abbreviations

V	Volt
V_{op}	Operating Potential
d	Spacing between atomic planes
θ	X-ray scattering angle
n	Positive integer
λ	Wavelength
ϵ	Mean size of crystalline domains
K	Dimensionless shape factor
β	Full width at half maximum of XRD peak

Li	Lithium
Ni	Nickel
Mn	Manganese
O	Oxygen
H	Hydrogen
C	Carbon

LIBs	Lithium-ion Batteries
redox	Reduction-Oxidation
LMNO	$LiNi_{0.5}Mn_{1.5}O_4$
PVP	Polyvinyl Pyrrolidone
SEM	Scanning Electron Microscopy
XRD	X-ray Diffraction
FWHM	Full width at half maximum

Chapter 1

Introduction

Over the past years there has been a rising interest in Li-ion batteries for electric vehicles, communication engineering and other applications. In order to fulfill the requirements that these applications bring with them new cathode materials are under investigation. To store as many energy as possible cathode materials with high operating potentials above 4.5 V vs. Li/Li$^+$ attract the most attention in the current Li-ion battery industry.

Many different cathode materials have been proposed, among which are $LiCoO_2$, $LiFePO_4$ and $LiMn_2O_4$. Of these materials spinel $LiMnO_4$ is de most promising, due to the low cost and the abundancy of the resources needed to produce it. However $LiMn_2O_4$ has poor cycling behaviour. For this reason many researches have been done on metal doped $LiMn_2O_4$. One of the most attractive materials is the material $LiNi_{0.5}Mn_{1.5}O_4$ or LMNO, because of its high theoretical capacity and operating voltage. [1]

A lot of ways to produce LMNO have been reported, such as solid-state reactions[2], co-precipitation[3] and sol-gel methods [4] and more. However, there are almost no reports of synthesis of LMNO by means of the electrospinning technique. With this technique one-dimensional nanofibers can be produced, which are highly beneficial for the cycling performance of the resulting Li-ion battery. By means of this nanostructuring technique, theoretically a high charge/discharge rate can be achieved. [1]

1.1 Goals and approach

The goal of this assignment is to find a method to produce LMNO nanofibers using the electrospinning method. To achieve this, a trial recipe is taken from literature and this recipe is improved until nanofibers can be produced with the solution. To improve the recipe observations and SEM images are used as input. Then, when a valid recipe is found the nanofibers are annealed and after that XRD is performed on the samples to investigate if indeed the correct composition is made. Also the effects of the annealing process on the morphology are investigated by again using observations and SEM imaging. This bachelor assignment has a strong emphasis on experimental work, due to the explorative nature of the research done.

Chapter 2

Theory

2.1 Lithium-ion Batteries

Lithium-ion Batteries(LIBs) make use of reversible electrochemical reactions to store and convert electrochemical energy. Using the discharging process as an example, the following steps can be identified (see Figure 2.1)[5]:

1. The electron and the Li-ion disassociate from the anode material at the same time and move towards opposite directions via solid-state diffusion.
2. The Li-ion moves towards the electrolyte and diffuses through it towards the cathode.
3. The electron passes through anode particles and their interfaces towards the current collector. It then travels through the external circuit towards the cathode and can then power a device.
4. Both electron and the Li-ion end up at the cathode material, again via solid-state diffusion.

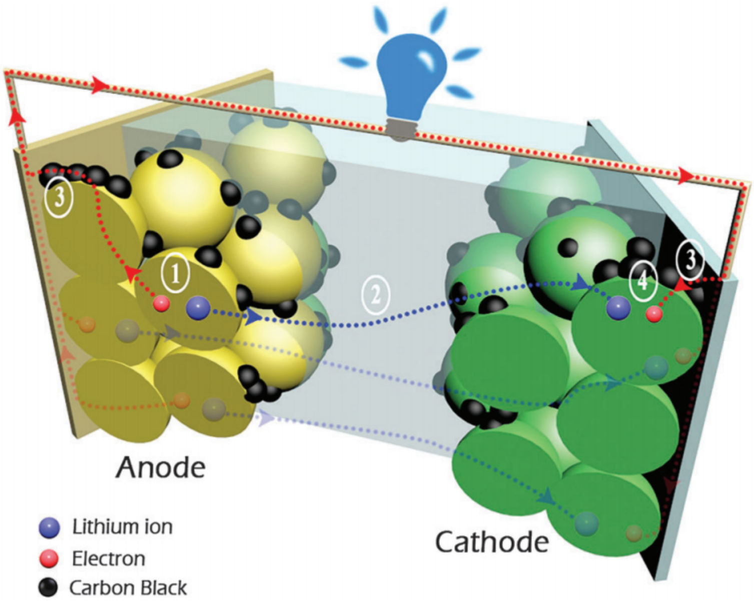

Figure 2.1: Transport pathways of the Li-ion and the electron in a LIB in the discharging process. The numbers indicate the different steps in the process. [5]

The electrochemical reactions in a LIB are redox reactions, which means that they have a certain reduction potential. The difference between these reduction potentials is often called the operating potential V_{op} and is a measure of the power that can be supplied by the battery. The operating potential is also partly determined by the Li-ion accommodation ability and the Li-ion and electron transport kinetics of the anode, electrolyte and cathode materials. One way of enhancing the performance of the LIB is thus by enhancing the transport kinetics of the Li-ions and the electrons. This can be done in a lot of ways, among which are nanostructuring and doping of the material, which are utilized in the case of electrospun $LiNi_{0.5}Mn_{1.5}O_4$. [5]

2.2 Material properties

A candidate material for a cathode in a LIB is $LiNi_{0.5}Mn_{1.5}O_4$ or LMNO. LMNO is a Nickel doped variant of the material $LiMn_2O_4$ and has a normal cubic spinel structure. A schematic representation of the spinel structure can be found in Figure 2.2. In the figure only the A and B sites of the molecule are indicated, but because the material is doped with nickel there are both nickel and manganese on the B-sites of the structure in a Mn:Ni ratio of 3:1.

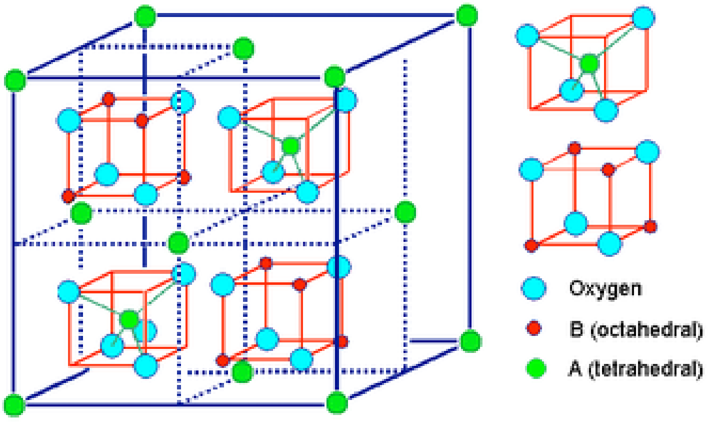

Figure 2.2: A graphical representation of the cubic spinel structure of an AB_2O_4 oxide. In case of $LiNi_{0.5}Mn_{1.5}O_4$ both Ni and Mn occupy B-sites(red) in the structure and Li occupies the A-sites(green).[6]

One of the reasons that LMNO is of interest as a cathode material is because of the cubic spinel structure. As a consequence this structure there are 3D lithium-ion diffusion paths, which improve the transport kinetics of the Li-ions. The Li-ions diffuse by moving from an 8a site towards an empty neighbouring octahedral 16c site, and then again towards an 8a site. [7] Because of these paths the ions can move through the material more easily, and thus faster. Because of this the material has a high intrinsic rate capability, which means that the battery will have high charge-discharge rates relative to materials with other structures. Another reason is the high theoretical capacity of 147 mA h g^{-1} that has been calculated for LMNO. [8, 9, 10]

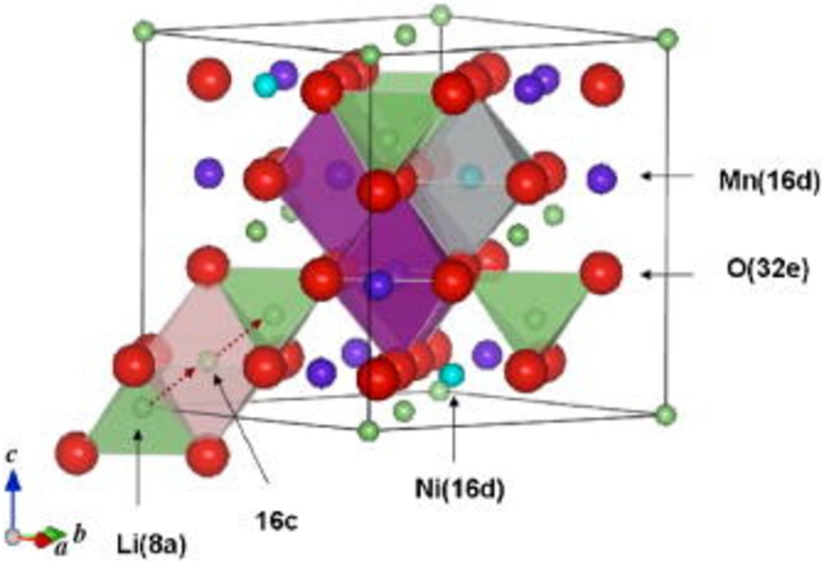

Figure 2.3: Diffusion path of lithium in the spinel $LiNi_{0.5}Mn_{1.5}O_4$. A possible diffusion path is indicated with the red arrows. [7]

The reason for the Nickel doping in LMNO is because pure $LiMn_2O_4$ has problems with its cycling behaviour. This is due to the fact that the $[MnO_6]$ octahedron in the material gets distorted during cycling. This results in a rapid capacity fading, which is undesired. To solve this the spinel is doped with nickel, which increases the strengths of the bonds in the octahedron. Because of these stronger bonds the material distorts less, which results in a smaller capacity fading. [11]

Although there are some major advantages to LMNO, there are also still some drawbacks to it. One of the main issues with LMNO is that also distortions occur during cycling. The electrochemical performance is negatively influenced by the fact that two phase transitions occur during cycling. The large lattice parameter difference between the different phases of LMNO cause the cathode to perform less due to the large volume change that this induces.[12] A possible solution to this problem could be the introduction of nanostructured materials. This is because nanostructured materials accommodate these volume changes more effectively than their bulk counterparts. [9]

Implementing nanostructuring in LMNO also has some additional advantages. It also improves the Li-ion transport kinetics of the material. This is due to the fact that the Li-ion diffusion length in the material drastically decreases, so the Li-ions have to diffuse over a smaller distance. This is because nanostructuring increases the specific surface area of the material, which means that the LMNO has more contact with the electrolyte. Because of this the interfacial reacting area is very high, which improves the transport kinetics. [9]

2.3 Electrospinning

In the last section it became clear that LMNO cathodes could be improved by nanostructuring techiques. A technique that has been researched a lot over the last couple of years is electrospinning. With this technique one-dimensional nanofibers can be produced. As stated before nanostructuring enhances the Li-ion transport kinetics by decreasing the Li-ion diffusion length. Also nanostructured LMNO accommodates the volume changes that occur during cycling better. Apart from these general advantages of nanostructuring, the electrospinning method has an additional advantage. In electrospinning a fiber mat is produced that is more flexible than the bulk material would have been. Because of this it may become possible to produce a flexible battery in the future.[5, 9]

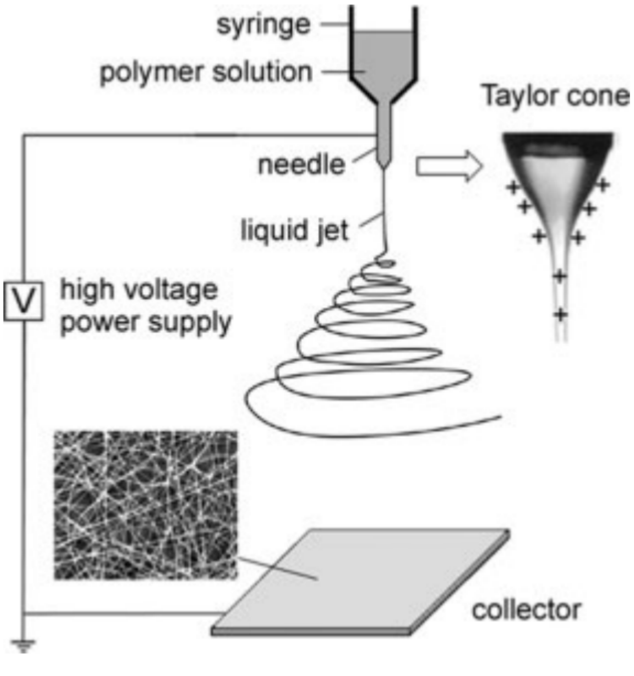

Figure 2.4: Schematic illustration of the basic electrospinning setup. The insets show a drawing of the Taylor cone and a typical SEM image of a electrospun layer of Polyvinyl pyrrolidone (PVP) nanofibers.[13]

The electrospinning setup consists typically of three main components: a high voltage power supply, a syringe pump containing a nozzle with a small opening and a grounded collector (see Figure 2.4). The principle of electrospinning is based on the interaction of a charged fluid with a strong electrical field. This charged fluid is a precursor solution that commonly consists of one or more precursor materials, containing the components of the desired product material, a sacrificial polymer template, that gives the solution its viscosity, and one or more solvents in which the other components are dissolved.

In the electrospinning process the precursor solution is pumped into the device by means of the syringe pump at a constant rate. When then a voltage is applied the interaction between the induced repulsion forces in the solution and the surface tension of the solution, causes the pendant droplet to deform at the tip of the needle. The conical structure that is formed is called the Taylor cone. When the applied voltage reaches its critical value, the repulsive electrostatic forces overcome the surface tension. Then a charged jet of the solution is ejected from the tip of the Taylor cone (see Figure 2.4).

This charged jet elongates and moves towards the collector in a straight line for a certain distance. Then it starts to bend and the jet is whipped around its axis by the electrostatic repulsion forces. These forces also elongate the jet further and make it become thinner. During this process the solvent is evaporated from the jet until it solidifies. Solidification happens when so much solvent is evaporated from the jet that the intermolecular forces become so large that it is no longer possible to further stretch the jet. The precursor/polymer nanofibers are collected on the grounded collector. Afterwards the sacrificial polymer is removed by sintering the film. [14, 15, 16, 17]

2.4 Parameters in the electrospinning process

There are a lot of parameters that influence the process and hence the product of the electrospinning procedure. These parameters fall into three main classes: Operation parameters, solution parameters and ambient parameters. Operation parameters are parameters in the set-up, such as the applied electric potential, the nozzle size, the flow rate of the solution and the tip-to-collector distance. Solution parameters include the viscosity of the solution, the precursor type, the electrical conductivity of the solution, the surface tension and the polymer architecture and concentration. The ambient parameters that influence the system are temperature, humidity and air velocity in the chamber. The most important parameters will be discussed in the following paragraphs.

2.4.1 Electric potential

One of the key parameters is the applied electric potential, due to the fact that it has a direct influence on the fluid flow. Changes in the electric potential influence the shape of the suspending droplet at the nozzle, its surface charge, the dripping rate of the solution and the velocity of the flowing solution. Because of this, the electric potential has a direct influence on the structural morphology of the produced film. [18] However previous studies have shown contradictory results. In some experiments the increase in electric potential resulted in an increase in the fiber diameter, but in other experiments it resulted in a decrease in the fiber diameter. Other studies showed that the influence of the electric potential on the produced film was relatively low compared to other parameters. [19]

This can be explained by the fact that two opposing processes are happening simultaneously. The decrease in fiber diameter can be explained by the fact that the stronger electric field induces larger electrical forces, which favour the formation of thinner fibers, because the jet gets elongated more due to these forces. Increasing diameter can be explained by the fact that a higher electric field can cause a higher flow rate, which leads to thicker fibers. This means that if the solution flow rate is kept constant, the increase in voltage will lead to a decrease in the diameter of the fibers. [20]

2.4.2 Nozzle size

The nozzle size also has influence on the diameter of the produced fibers. Several studies reported a concave relationship between the size of the nozzle and the diameter of the fiber. The increase in nozzle size causes an increase in the fiber diameter up to an optimum and after that the diameter decreases again. This is due to the fact that large fibers can split in multiple smaller fibers easily, which of course decreases the diameter again. [20, 21]

2.4.3 Flow rate

The effect of the flow rate on the morphology of the fibers is not very significant. It has been observed that the diameter of the fibers will increase slightly when the flow rate is increased. Aslo there is a minimal value for the flow rate, because if it is too small it is not possible to establish an equilibrium Taylor cone and no continuous fibers will form on the collector. There is also a maximum in the flow rate, because the jet will not be stable anymore when the flow rate is too high. This is due to the fact that then more solution gets delivered to the nozzle than can get removed by the jet with the induced electrical forces. If that happens the jet will no longer be stable and no uniform fibers will form and also droplets will end up on the collector, where they will form large beads.[3, 22]

2.4.4 Tip-to-collector distance

Another important parameter is the tip-to-collector distance. The larger this distance is, the longer the jet has the time to dry and solidify. If the tip-to-collector distance is too low, the fibers cannot dry in time and the wet fibers will land on the collector. Then the fibers will fuse and form a network in stead of separate fibers and also lots of beads are formed. The larger this distance, the longer the time that the fiber can dry in the air and thus the lower the number of beads in the fibers at the collector. However if the tip-to-collector distance is too high, the electric field between the tip and collector will not be large enough to facilitate electrospinning.[19]

2.4.5 Viscosity

Another parameter that governs the morphology of the produced film is the viscosity of the solution. If the viscosity of the solution is low, the fibers will be small in diameter and show beads. When the viscosity increases, the fibers will become thicker and the amount of beads decreases and merges with the thickening fiber to form smooth fibers.

If the viscosity is too low, the solution will not keep together to form a stable Taylor cone, but will in stead spray in droplets from the nozzle. In that case one no longer speaks of electrospinning, but rather of electrospraying. This is due to the fact that the lower the viscosity is, the easier it is for the electrical forces to stretch the jet. The more the jet is stretched, the smaller the diameter of the fibers will get, up to the point that the jet can be pulled apart completely, which happens in the case of electrospraying. The viscosity of the solution is mostly dependent on the concentration of the polymer in the solution. The more polymer is added to the solution, the more viscous the solution gets.[20, 23]

2.4.6 Polymer concentration

Next to its contribution to the viscosity, as discussed in the previous section, the concentration of the polymer in a precursor/polymer/solvent solution also has another function. It determines the length and stability of the resulting fibers. This is due to the fact that during the sintering process the polymers are removed from the film and only the desired composition remains. A high weight ratio of the polymer results in an incompact dispersion of the nanoparticles of the desired compound, which makes that the nanofibers tend to break into shorter nanorods. However a reduced amount of the polymer helps to construct long continuous fibers. [14]

2.4.7 Solvent concentration

Another parameter that influences the morphology of the resulting fibers is the solvent concentration. When there is a high amount of solvent in the solution it takes a longer time to evaporate the solvent from the fiber. If the amount of solvent is too high the fibers are still wet when they arrive at the collector. This leads again to the formation of beads. [19]

2.4.8 Electrical conductivity

The diameter of the fibers is also depending on the electrical conductivity of the solution. It has been observed that the diameter of the spun fibers were smaller when the electrical conductivity was higher. This is because then the fibers can be stretched by the electrical forces more easily. When the electrical conductivity is low, more beads can be observed in the fiber. This is most likely due to the fact that the jet cannot be elongated well by the electrical forces due to the applied electrical field, because of this low conductivity. This can be avoided by using longer polymer chains, thus polymers with a higher average molecular weight, in the solution.[24]

2.4.9 Room humidity

The room humidity also has an effect on the formation of the fibers. This is due to the fact that the jet absorbs water from the surroundings during the process. When the humidity is higher, the partial pressure of the water in the air is higher, which leads to stronger absorption of the water from the air into the jet. Because of this it takes a longer time to solidify the jet into a fiber and when the humidity is too high, the jet has not dried completely yet when it arrives on the collector. If that happens, no good fibers will form, because the fibers fuse and form lots of beads and cross linked fibers, which is not desirable. On the other hand, if the humidity is high, but not too high, the elongation process can continue longer before the fiber solidifies, which results in fibers with a smaller diameter. [17]

2.4.10 Temperature

There are two main effects that the temperature has on the electrospinning process. The first effect is the evaporation rate of the solvent. The rate increases exponentially with increasing temperature. The higher the temperature, the faster the solvent evaporates and thus the shorter the elongation process can take place. Therefore the diameter of the fibers increases with increasing temperature.

The other, opposing process is the rigidity of the polymer chains. These have more freedom to move when the temperature is higher, which causes a lower viscosity. The lower the viscosity, the more the jet can be stretched and the smaller the diameter of the fibers will become, as stated before in Section 2.4.5. [17]

2.5 X-ray Diffraction

In this study the material produced is going to be determined using X-ray Diffraction or XRD. This analysis technique makes use of Bragg diffraction of X-rays on crystal lattices. Bragg diffraction occurs when the wavelength of the incident X-rays is comparable to the atomic spacing of the lattice. Constructive interference occurs when the Bragg's law is fulfilled and a peak in intensity occurs. The Bragg's law is given by[25]:

$$2d \sin\theta = n\lambda \tag{2.1}$$

In this equation d is the spacing between atomic planes;
θ is the scattering angle or angle of incidence(see Figure 2.5);
n is a positive integer;
λ is the wavelength of the incoming X-ray.

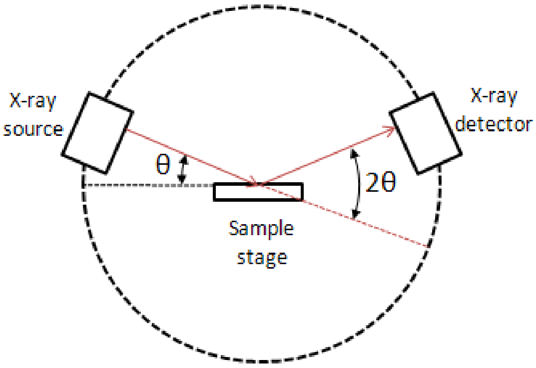

Figure 2.5: A simplified XRD setup with the angles θ and 2θ specified.[26]

A common way to display an XRD spectrum is by plotting the angle 2θ against the intensity at that angle. In this way for every material a specific line spectrum is found. A sample can then be compared to known material spectra to determine the sample material. Also information about the crystallinity can be found in the XRD spectrum. The size of the domains in the sample can be described by Scherrer's Equation, which can be written as[27]:

$$\epsilon = \frac{K\lambda}{\beta\cos\theta} \tag{2.2}$$

In this equation ϵ is the mean size of the crystalline domains;
K is a dimensionless shape factor, with a value close to unity. The shape factor has a typical value of about 0.9, but varies with the actual shape of the crystallite;
λ is the wavelength of the incoming X-ray;
β is the full width at half maximum (FWHM) of the peak under investigation;
θ is again the scattering angle at which the peak under investigation is found.

As can be seen in Equation 2.2 the mean size of the crystalline domains is inversely proportional to the FWHM of the peak that corresponds to these domains. Thus, the broader the peak is and thus the larger the FWHM, the smaller the crystalline domains are. Also it can be seen that for larger angles of θ the FWHM increases. It is therefore expected that the peaks become broader for larger θ.

Chapter 3

Experimental work

There are several processes involved in the production of electrospun LMNO nanofibers. In this chapter the experimental work is presented to produce and characterize such nanofibers.

3.1 Solution preparation

Firstly the solution has to be prepared that is going to be used in the electrospinning process. This is done by mixing the precursors, solvents and polymers together in the correct order and quantities. There are several ways to produce a precursor solution for LMNO. In this case as precursors powders of lithium hydroxide(LiOH), nickel acetate tetrahydrate ($Ni(CH_3COO)_2 \cdot 4\,H_2O$) and manganese acetate tetrahydrate ($Mn(CH_3COO)_2 \cdot 4\,H_2O$). As solvents water ($H_2O$), acetic acid($CH_3COOH$ and isopropanol ($i{-}C_3H_7OH$) are used. The polymer powder used is Polyvinylpyrrolidone K-90 (PVP K-90) which has an average atomic weight of 360.000. The molar ratio of these compounds can be found in Table 3.1. Only for PVP the molar ratio is not shown since it is extremely small in comparison to the other values ($\sim 10^{-6}$) due to its extremely high atomic weight. The used recipe for the solution is adapted from a recipe to produce LMNO by the sol-gel method by Hoshina et al. and is further adapted to produce nanofibers of the correct structure and composition. [4]

Table 3.1: The different components and their molar ratio's in the solution. Also the order of addition is specified. The molar ratio of the PVP is not specified because it is extremely small compared to the rest of the molar ratio's due to the extremely high molar weight.

Component	Molar ratio	Order of addition
LiOH	1	6
$Ni(CH_3COO)_2 \cdot 4\,H_2O$	0,5	2
$Mn(CH_3COO)_2 \cdot 4\,H_2O$	1,5	4
PVP K-90		7
$i{-}C_3H_7OH$	40	5
CH_3COOH	45	3
H_2O	70	1

To produce a solution in which all powders are dissolved properly it is important to mix all substances in the correct order. First the nickel acetate tetrahydrate is weighted and dissolved in the water. The solution is stirred with a stirring magnet until all the powder is dissolved.

Next the acetic acid is added to the solution. Also the manganese acetate tetrahydrate is added and again the solution is stirred until all powder is dissolved. This may take a couple of minutes. Then the isopropanol and the lithium hydroxide are added to the solution and again the solution is stirred until all is dissolved.

Lastly the PVP K-90 is added to the mixture. This probably causes the PVP to clot at first. This is not a problem since the PVP will dissolve eventually when stirred for a couple of hours. The solution has to be stirred continuously until it is used for the electrospinning process. After a couple of days the solution will become unstable and the Nickel will precipitate from the solution. When this has happened the solution is no longer usable and a fresh solution should be prepared. The time of stability of the solution can be elongated by storing the solution on a hot plate at 80°C.

3.2 Electrospinning

When the solution is prepared, it can be used in the electrospinning process. This can be done in the following way. First the solution has to be cooled down to room temperature, if it has been stored on the heating plate. Then, the needle has to be checked for blockades that can occur due to earlier experiments. This can be done by means of a small metal wire that is put through the nozzle of the needle.

Next the needle is attached to a plastic tube and they both are cleaned using disposable syringes. This can be done by first filling a syringe with ethanol and flush the tube and needle with it. When the syringe is empty it is detached and filled with air, which is then put through the tube to eject all the remaining ethanol. After that a new syringe is filled with approximately 1 ml of the prepared solution and the tube and needle are flushed again, this time with the solution. Then the tube is flushed with air another time to also delete the solution from the tube again. After this the system is ready for experiments.

The syringe in which the solution was for cleaning is filled again with approximately 2 mL of the solution. Then the syringe is held upside down and it is gently emptied in a beaker up to the point that all air has left the syringe and the tube and only solution is in the tube. This is important because it ensures that there will be a constant flow of solution without air bubbles in between. Then the syringe is mounted on the syringe pump and the needle is placed into its holder which is attached to the voltage source.

Next the collector plate is prepared with a layer of aluminum foil, which is connected to the voltage source as well. It is possible to deposit the fibers on the aluminum foil, if it is not the intention to anneal them. Otherwise a silicon wafer is put on the aluminum foil with scotch tape on the back of the wafer, while making sure there is a good contact between the aluminum and the wafer, so the wafer is still connected to the voltage source. If it is necessary to remove the fiber mat from the collector afterwards, a nice trick is to spin on laboratory blue paper. This can be attached with scotch tape on the collector that is covered in aluminum foil.

Then the tip-to-collector distance is set by tuning the distance between the needle and the collector plate. Then the syringe pump is set to the correct flow rate and the voltage source is turned on. Now deposition of the fibers starts.

When the deposition is finished, the syringe pump is stopped again and the voltage source is turned down to zero and then shut down. Lastly the sample is removed from the collector plate and the plastic tube and the needle are cleaned thoroughly with ethanol again to remove the solution from them.

3.3 Annealing

After the electrospinning process the sample needs to be annealed. Annealing is the process where the sample is heated to a certain temperature which is then maintained for some time after which the sample is cooled again. In the annealing process the sacrificial polymer is burned out of the sample and the LMNO crystals form. Eventually only the LMNO fibers are left.

This can be done in two ways. The first is by means of a conventional oven. The sample is placed into the oven and heated to 800°C with 500°C/h. Then it is held there for 15 minutes. After that the sample is cooled again passively and the sample can be removed from the oven. The temperature of 800°C was chosen to be the same as the annealing temperature in the recipe of Hoshina et al. [4]

The other way is by using a 1000 Watt microwave oven. In this kind of oven the temperature is increased locally as fast as possible to 800°C with approximately 3200°C/h. In this way the sample is shock heated and the temperature is maintained for 2 hours at that temperature. After that the sample is cooled again to room temperature. The advantage of this method is that it is much faster than the conventional method, which causes all PVP to burn out at the same time. On the same time the LMNO crystallizes, and sinters together into nanofibers.

Chapter 4

Results

4.1 PVP concentration

As stated before the solution is tuned to produce nanofibers. To be able to produce nanofibers it is important to make use of the correct amount of PVP in the solution. From theory it has been shown that PVP plays an important role in the viscosity of the solution and therefore in the production of the nanofibers. With the correct concentration PVP in the solution the fibers will be long and show little beads (see Section 2.4.5). Therefore several solutions with different concentrations of PVP are made and electrospun (see Table 4.1). In this series of experiments the concentration of PVP was gradually increased until the point that the fibers were smooth and continuous. For every solution with a specific concentration of PVP the distance and the voltage were varied to make sure that the best possible fibers were obtained with the current solution. This was tested by making SEM images of the samples produced as well as by observations done during the electrospinning process.

Table 4.1: The different components in the solutions where the PVP concentration was varied.

Component	Amount mL	Amount gram
LiOH		0.0479
$Ni(CH_3COO)_2 \cdot 4\,H_2O$		0,249
$Mn(CH_3COO)_2 \cdot 4\,H_2O$		0,735
$i{-}C_3H_7OH$	6,1	
CH_3COOH	5,5	
H_2O	2,5	

Several different amounts of PVP were used in the solution, namely 0.4 gram, 0.7 gram, 0.8 gram, 0.9 gram and 1.0 gram. Each different solution was tested as said and the resulting sample was put into the SEM to determine the morphology. The most important observations from these solutions can be found in Table 4.2. All samples excluding the one from the solution with 0.4 grams of PVP were put into the SEM. Figure 4.1 clearly shows a couple of beads that were formed with the solution containing 0.7 grams of PVP, which indicated that the amount of PVP was too low. Also it was observed that droplets were falling from the needle onto the sample continuously, which was also an indication that the viscosity was too low , and thus the PVP concentration had to be increased.

In Figure 4.2 a SEM image of one of the samples made with the solution with 0.8 gram of PVP can be seen. The brighter spots on the sample are small droplets that fell on this sample, which is unwanted. This could however not be observed with the naked eye. No droplet was falling from the needle while this was happening. This indicates that the viscosity was too low still to facilitate a stable jet, which is used to make long and continuous fibers. However in this sample almost no beads were observed.

Table 4.2: The optimal values for the potential, the tip-to-collector distance and the flow rate to produce the best sample and the observations that were done during deposition for the solutions with the different PVP concentrations.

PVP amount	Optimal conditions			Observations
0.4 gr	17 kV	18 cm	0.5 mL/h	Very low viscosity, No deposition
0.69 gr	17 kV	18 cm	0.5 mL/h	Drips, beads
0.8 gr	15 kV	18 cm	0.3 mL/h	Droplets on sample
0.9 gr	15 kV	18 cm	0.3 mL/h	Good deposition, long continuous fibers
1.0 gr	15 kV	18 cm	0.3 mL/h	Good deposition, long continuous fibers

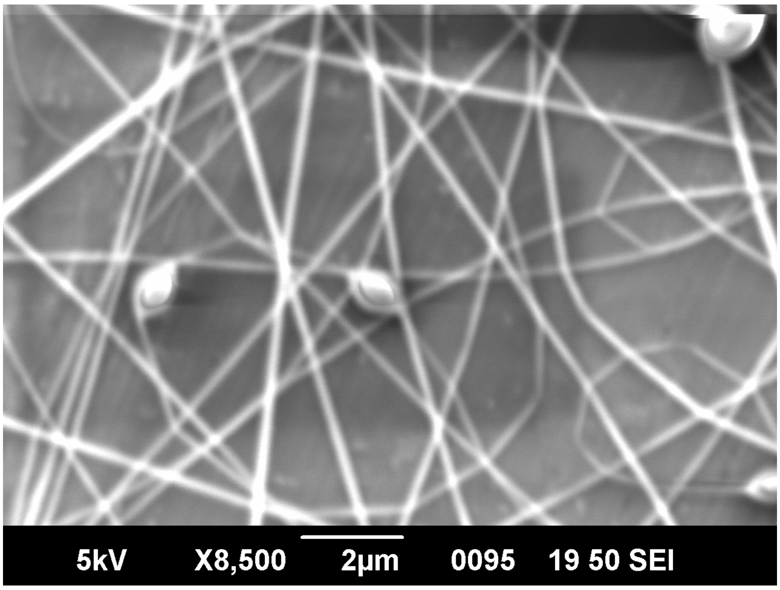

Figure 4.1: A SEM image of electrospun fibers with beads. This sample was made with the solution with 0.7 grams of PVP.

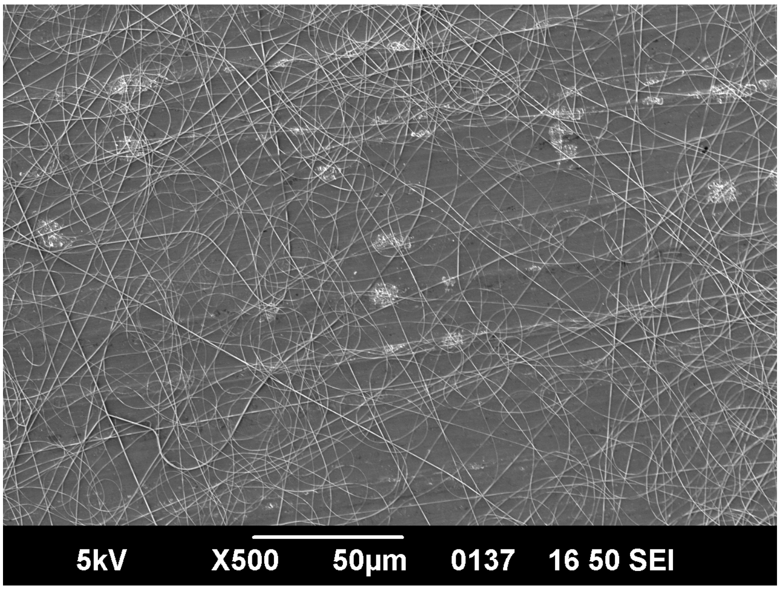

Figure 4.2: A SEM image of droplets on a fiber mat. The bright spots are the droplets that have fallen on the sample. This sample was made with the solution with 0.8 grams of PVP.

Finally the two solutions with 0.9 grams and 1.0 grams of PVP were tested. With both solutions good samples with long continuous fibers were obtained (see Figure 4.3). Almost no beads were found on the samples made with both solutions. Both solutions are good candidate solutions to prepare LMNO nanofibers. It was observed however, that a large droplet was slowly forming at the tip of the needle. When left alone, this droplet would spread all over the sample and ruin it. To avoid this, the droplet was regularly removed from the tip with standard blue paper from the lab. In this way the droplets would not end up on the sample and ruin it.

The difference between the 0.9 gram PVP solution and the 1.0 one is that the 1.0 grams solution would produce small grains on the sample when the sample was spun for a long time (longer than 15 minutes). This is probably because of the high PVP saturation in the solution, which makes the solution instable.

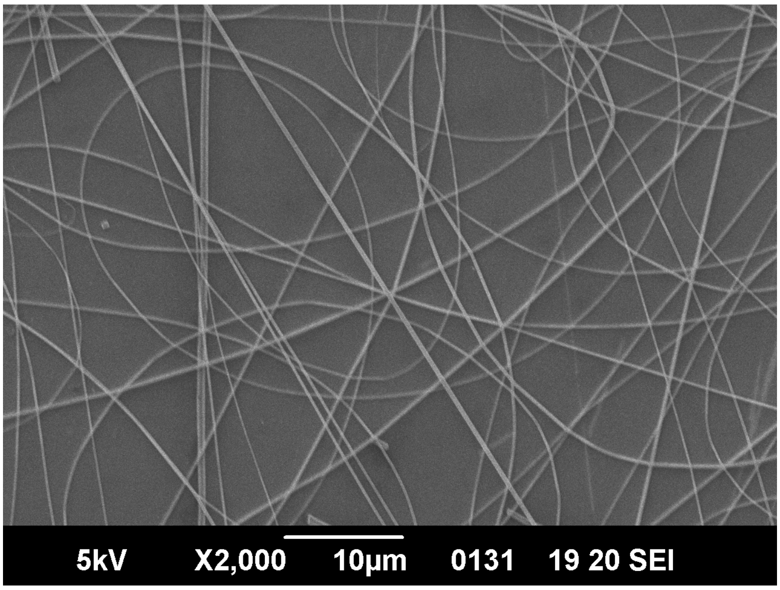

Figure 4.3: A SEM image of a fiber mat produced with the solution containing 0.9 grams of PVP. The fibers are smooth and continuous.

4.1.1 Conclusion

It has become clear from experiments that the best PVP concentration in this solution would be 0.9 grams of PVP. This is because of its good deposition and because the produced fibers were long, smooth and continuous. Also the fiber mats that were spun with the 0.9 grams solution could be spun for a long time without problems.

4.2 Annealing

As stated before in Section 3.3, there were two ways of annealing the samples produced with the electrospinning method. The conventional oven and the microwave oven method. Both have their advantages and their disadvantages in production of LMNO nanofibers.

The conventional oven can contain larger samples than the microwave oven. Because of this, the samples that were spun on large wafers were annealed with the conventional oven. These wafers could then be investigated with the XRD, of which the results are presented in the following section.

It was found however that samples that were very thick did not survive the treatment in the conventional oven. Somewhere in the process these samples burned, which resulted in a destroyed sample. It could clearly be seen that the places where the sample was very thick, the fiber mat is completely gone (see Figure 4.4).

This could be explained by the fact that when the PVP is burnt out of the sample the resulting heat has to go into the atmosphere. However if the sample is too thick this becomes much harder to do. The heat of the bottom layer of the nanofibers has no place to go and the sample becomes hotter and hotter, which eventually leads to a flame on the sample which burns the complete sample and thus destroys it.

On the other hand it can be seen in Figure 4.4 that thinner samples are also cracking when annealed. The fiber mat gets ripped apart due to the fact that it shrinks while it is attached to the wafer. This is not a big issue in this experiment, but in future research this could propose problems.

It was also tested what the effect was of the different approaches for annealing. In Figure 4.5 the difference between the two samples can be seen. Sample A was annealed with the microwave oven while sample B was annealed with the conventional oven method. The result shows that the fibers on the sample annealed with the microwave oven are still smooth and continuous, while the fibers on the sample annealed with the conventional oven have broken up into smaller sections and the fibers themselves are not smooth anymore.

A reason for this could be that the microwave oven heats the sample to 800°C much faster than the conventional oven. Because of this shock heating process everything burns out at the same time which makes sure that the fibers are sintered together in a single uniform process. This ensures that

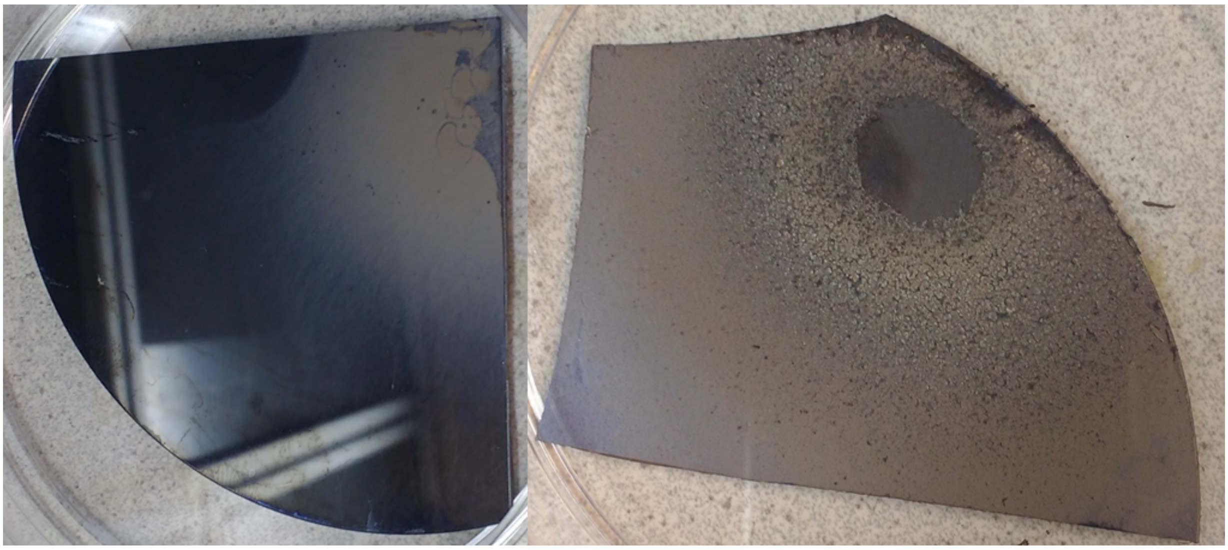

Figure 4.4: A comparison between two annealed samples by means of a conventional oven. The sample on the left was spun for 2,5 minutes and the right sample was spun for 45 minutes. It can be clearly seen that the right sample was burnt during the annealing process, while the left one was not.

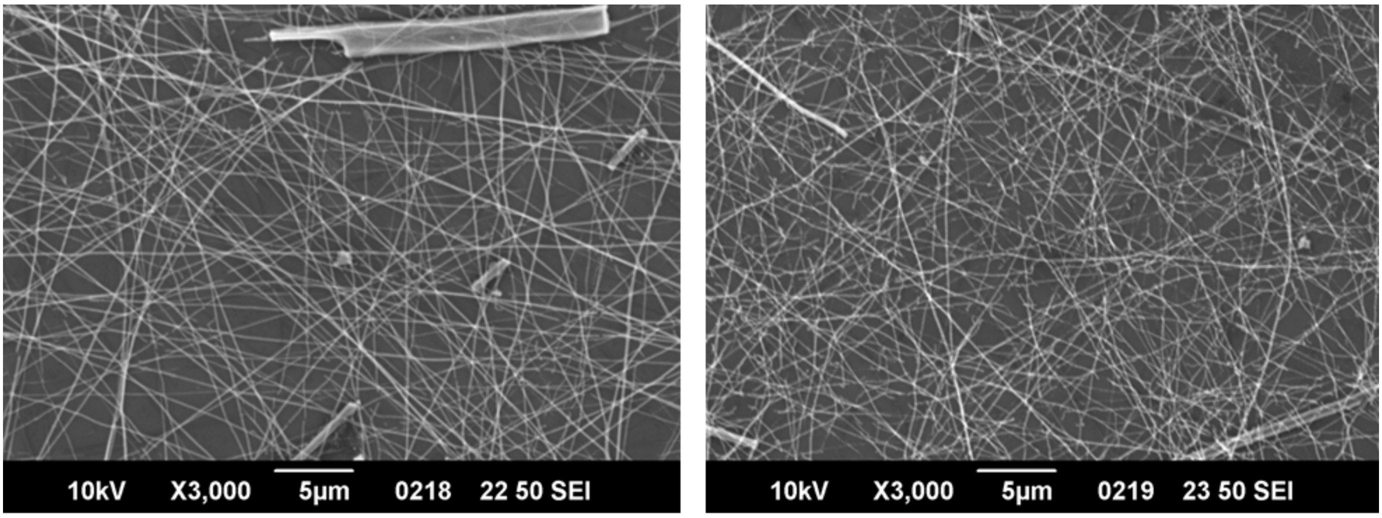

A.

B.

Figure 4.5: SEM pictures of two annealed samples . Sample A was annealed using the microwave, while Sample B was annealed with the conventional oven.

the fibers keep their form and stay smooth and continuous. On the other hand, the fibers that were annealed with the conventional oven method are only sintered slowly, so the fibers are starting to sinter together already, but still parts of the PVP and the acetate is burning out. Because of this the fibers do not anneal uniformly and this causes the fiber to break up in shorter pieces an to be less smooth overall.

4.2.1 Conclusion

It is possible to anneal the fiber mats produced with the PVP containing solution, while keeping the nanofibers intact, which was important. However, it has become clear that still a lot needs to be done to improve the annealing process, to reach the goal to produce thick fiber mats with smooth fibers. Thick fiber mats get severely damaged with the current annealing process. Also thin fiber mats get ripped apart when they are annealed while they are still attached to the wafer.

4.3 X-ray Diffraction

To determine if indeed LMNO nanofibers have been produced XRD measurements have been carried out. Because the samples produced with the electrospinning method are very thin, the measurements needed to be done for a very long time to get clear peaks in the XRD spectrum. For the measurement from which the spectrum is shown in Figure 4.6 the time of measurement was 15 hours, which is very long for an XRD scan. The 2θ scan was carried out for the range of 15 to 66 degrees. A 20 points average filter has been used to reduce the noise of the measurement, such that the peaks could be seen more clearly. Furthermore the program Highscore Plus was used to determine the exact location of the peaks and to determine the materials that were present in the sample.

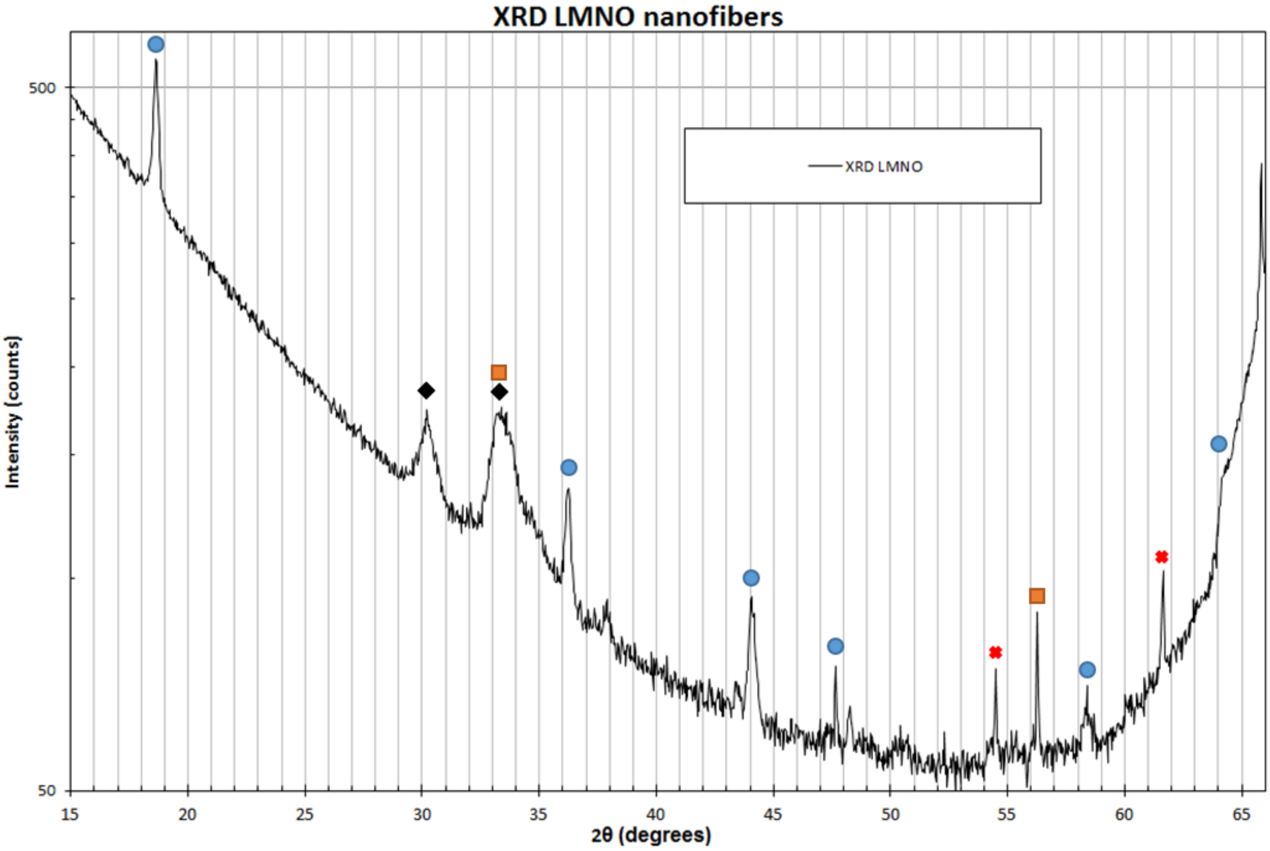

Figure 4.6: XRD spectrum of an annealed sample with LMNO nanofibers with labels above the peaks that indicate the different phases, namely LMNO (blue dots), $LiOH \cdot H_2O$ (black rhombi), Li_2O (orange squares). The unidentified peaks are labeled with a red cross.

A list of peaks found with Highscore Plus can be found in Table 4.3 with the material they are indicative for. These peaks also have been tagged with a different symbol for every material in Figure 4.6. A bar graph of XRD spectra of the different sample components can be found in Figure 4.7. As can be seen the most prominent peaks in the LMNO spectrum are also present in the sample spectrum. This indicates that the sample does contain LMNO nanofibers, which was what was intended. It can be seen that the relative intensity of the different crystal orientations is different for the sample compared to the LMNO spectrum. This could be because the sample is very thin and therefore the relative intensities are different than their bulk counterparts.

There is also another phase found in the sample. There are two candidate materials for this phase. These materials are Li_2O and $LiOH \cdot H_2O$. It is also possible that a combination of the two materials is found in the sample. It could be however that even another material is present in the sample, but no other candidates could be found that matched these peaks. All the known combinations of Li Ni Mn and O in the database have been compared to the sample spectrum, and the shown candidates were the best matches.

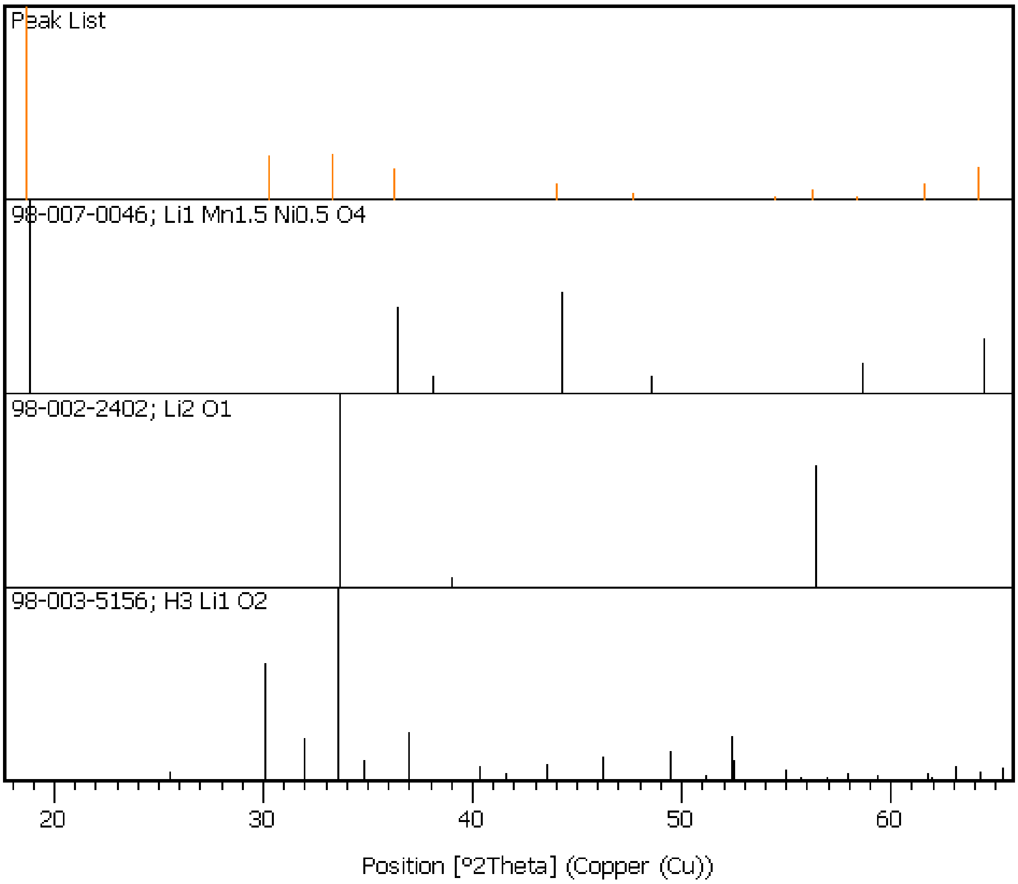

Figure 4.7: A bar chart containing the sample spectrum and the spectra of the candidate materials that the sample peaks indicate. From top to bottom the charts are of the sample, LMNO, Li_2O and $LiOH \cdot H_2O$.

Table 4.3: A table containing all identified peaks in the spectrum with the material they are indicative for.

2θ	**Indicative for**
18,6367	LMNO
30,2191	$LiOH \cdot H_2O$
33,3394	$LiOH \cdot H_2O$, Li_2O
36,2351	LMNO
44,0544	LMNO
47,6585	LMNO
54,4422	No match found
56,2651	Li_2O
58,3954	LMNO
61,6246	No match found
64,2181	LMNO

As can be seen in Figure 4.6, the peaks indicative for LMNO are rather sharp, whereas the peaks indicative for the second phase are more broad. In section 2.5 the relation between FWHM or broadness and the morphology of the sample was described by Equation 2.2. The broader peaks of the second phase thus indicate that the second phase is not continuous throughout the material, but rather the crystalline domains are small. Therefore it is likely that thes impurities are present in small islands all over the sample. On the other hand the peaks for LMNO are rather sharp, which means that the material has large crystalline domains. This is an indication that the LMNO is more continuous throughout the material.

The intensity of the peaks tells something about the amount of material that is present in the sample. As can be seen in Figure 4.6, the intensity of the LMNO peaks is larger than those of the second phase peaks. This indicates that the LMNO is more abundant in the sample than the second phase. The intensity of the second phase is however also quite high, so probably the amount of second phase is quite high in the sample.

4.3.1 Conclusion

From the XRD spectra it can be concluded that the annealed samples do indeed contain LMNO. There is however a second phase present. It was found that the XRD spectra of Li_2O and $LiOH \cdot H_2O$ coincide with the peaks of the second phase. It is therefore very likely that the second phase consists of these two components. From the FWHM of the peaks it could be deducted that the LMNO was present throughout the sample, while the second phase was more localized in small domains. Lastly, the intensity of the LMNO peaks is larger than that of the second phase, which indicates that there is more LMNO than second phase. However, the second phase peaks are still quite large, so there is probably quite a lot of second phase present.

Chapter 5

Discussion & Recommendations

5.1 Discussion

Over the course of this Bachelor assignment there were several things that could have gone better. The first is that it was unclear in the beginning that the PVP would settle on the bottom of the bottle after some time. It was assumed that the solution was no longer usable when this would happen. After some time it was discovered that the solution should be stored on a heat plate at 80°C. When this was done, the solution was stable for a longer time and could thus be used for a longer time. Therefore the time put into constantly remaking a solution could have been severely decreased, which would have left time to do more experiments.

Also, sometimes the time it took to weigh the LiOH was too long. It could be seen that if no extra LiOH was added the balance would still slowly show an increase in the amount of material. This indicates that the LiOH reacts with water in the air and then gains weight. If the time between weighing and adding to the solution would be decreased it could decrease the contamination of the solution. Maybe the amount of $LiOH \cdot H_2O$ would not have been as high as it was in the current set of samples.

Another thing that could have influenced the result is that the annealing temperature of 800°C was taken from the recipe of Hoshina et al. without further extensive analysis. This could explain the burning of the samples and therefore it would have been a good idea to do experiments on the correct annealing temperature. Due to time shortages this was not done in this study.

Furthermore, the XRD spectra contained quite some noise. The sample could have been calibrated even better. Also another slit, for example the $1/32°$ slit in stead of the $1/16°$ slit, could have been used, which reduces the noise even further. Next to that the scans performed with the XRD could have been done over a larger interval, such that a larger part of the spectrum could be analyzed using Highscore Plus. Now only a scan was performed up to 66 degrees. Because of this some peaks fell out of the range, which could have held more information on the materials in the sample.

A last thing that is not included in this research is the influence of the room humidity and the temperature. Over the months that this study was done, the temperature and humidity could have shifted a lot. This was not measured and therefore this could have had some unwanted consequences, which would have decreased the reproducibility of the sample production. However, the effects of room humidity and temperature are not very large, so probably the study is not influenced a lot by this.

5.2 Recommendations

There is still a lot that can be investigated in the production and the material properties of LMNO nanofibers. Firstly, it is important to be able to produce LMNO nanofibers without having a second phase. To check if the second phase is indeed consisting of $LiOH \cdot H_2O$, a different precursor for Lithium can be used. A good example of this is $CH_3COOLi \cdot H_2O$, which was also used by Hoshina et al.[4] but was not available at the labs at the time. If this precursor is used, there is no LiOH present and thus it could not appear as a second phase.

Also new ways of producing a precursor sol could be investigated. While this research was almost finished, a novel study by Zhong et al.[1] was published which provides an alternative way of producing LMNO nanofibers. Different solvents have been used and also the order of addition is quite different from what has been done in this study.

Furthermore the annealing process is different in the study by Zhong et al.[1] and takes place at lower temperatures than in this study, which could maybe solve the issues that have been encountered during this study. Of course, a starting point could be to just test if the samples turn out less damaged at lower temperatures. Another possibility is to anneal the samples by turning up the heat very slowly. This is however very time consuming, and therefore maybe not ideal.

Aditionally, to gain more insight in the correct annealing temperature Thermogravimetry and Derivative Thermogravimetry could be used. These techniques measure the weight of the sample as a function of the temperature. From this the temperature can then be deduced where the PVP burns out, but the LMNO will not.

Of course it is also interesting to find out what the electrochemical properties of such fiber mats are. Future research could go into the characterization of the LMNO fiber mats. With cyclic voltammetry the cyclic behaviour of the LMNO nanofibers can be investigated. In this way it can be checked if the fiber mat does indeed perform better than the bulk material.

Another interesting thing that could be investigated is the flexibility of the fiber mats, since it would be interesting to see if a flexible cathode could be prepared from electrospun LMNO. If that is possible it could lead to the development of a flexible battery in the future.

Chapter 6

Conclusion

This thesis started with a literature study into LIBs, electrospinning and the parameters involved there, LMNO and XRD as a starting ground to be able to produce LMNO nanofibers by electrospinning. Afterwards the experimental setup was determined in chapter 3. Then the experiments were carried out and the results and partial conclusions about these experiments are described in chapter 4. Then, chapter 5 contained a discussion of the obtained results and an outlook for future research. Lastly, this chapter serves as a summery of the conclusions that followed from the results of this study.

It has become clear from experiments that the best PVP concentration in the solution prepared in this study is 0.9 grams of PVP. This is because of its good deposition and because the produced fibers were long and continuous. Also the fiber mats that were spun with the 0.9 grams solution could be spun for a long time without problems.

Furthermore, annealing the produced fiber mats while keeping the fibers intact revealed to be a challenge. The best annealing process thus far is shock heating the sample by using a microwave oven. In this way the fibers stay smooth and continuous.

Additionally, thick fiber mats get severely damaged with the current annealing process, while thin fiber mats get ripped apart when they are annealed while they are still attached to the wafer.

Also, from the XRD spectra it can be concluded that the annealed samples as prepared in this study do indeed contain LMNO. There is however a second phase present. It was found that the XRD spectra of Li_2O and $LiOH \cdot H_2O$ coincide with the peaks of the second phase. It is therefore very likely that the second phase consists of these two components. From the FWHM of the peaks it can be deduced that the LMNO is present throughout the sample, while the second phase is more localized in small domains.

Lastly, the intensity of the LMNO peaks is larger than that of the second phase, which indicates that there is more LMNO than second phase. However, the second phase peaks are still quite large, so there is probably quite a lot of second phase present.

To conclude, this thesis can be seen as a first step towards the production of LMNO nanofibers with the method shown. There is however still much more work to do before these LMNO fiber mats can be used in Li-ion Battery applications.

Bibliography

[1] Shengkui Zhong, Piao Hu, Xia Luo, Xiaoping Zhang, and Ling Wu. Preparation of $LiNi_{0.5}Mn_{1.5}O_4$ cathode materials by electrospinning. *Ionics*, pages 1–8, 2016.

[2] Nader Marandian Hagh and Glenn G. Amatucci. A new solid-state process for synthesis of $LiNi_{0.5}Mn_{1.5}O_{4-\delta}$ spinel. *Journal of Power Sources*, 195(15):5005 – 5012, 2010.

[3] Shu Zhang, Woo Sub Shim, and Jooyoun Kim. Design of ultra-fine nonwovens via electrospinning of nylon 6: Spinning parameters and filtration efficiency. *Materials & Design*, 30(9):3659 – 3666, 2009.

[4] Keigo Hoshina, Kazuomi Yoshima, Masashi Kotobuki, and Kiyoshi Kanamura. Fabrication of $LiNi_{0.5}Mn_{1.5}O_4$ thin film cathode by {PVP} solgel process and its application of all-solid-state lithium ion batteries using li1 + xalxti2 x(po4)3 solid electrolyte. *Solid State Ionics*, 209210:30 – 35, 2012.

[5] Yuxin Tang, Yanyan Zhang, Wenlong Li, Bing Ma, and Xiaodong Chen. Rational material design for ultrafast rechargeable lithium-ion batteries. *Chem. Soc. Rev.*, 44:5926–5940, 2015.

[6] Spinel, perovskite, and rutile structures. `http://chemwiki.ucdavis.edu/Textbook_Maps/Inorganic_Chemistry_Textbook_Maps/Map%3A_Inorganic_Chemistry_(Wikibook)/Chapter_08%3A_Ionic_and_Covalent_Solids_-_Structures/8.6%3A_Spinel,_perovskite,_and_rutile_structures`, accessed on 22-4-2016.

[7] H. Xia, Y. S. Meng, L. Lu, and G. Ceder. Electrochemical properties of nonstoichiometric $LiNi_{0.5}Mn_{1.5}O_{4-\delta}$ thin-film electrodes prepared by pulsed laser deposition. *Journal of The Electrochemical Society*, 154(8):A737–A743, 2007.

[8] Kuppan Saravanan, Angelique Jarry, Robert Kostecki, and Guoying Chen. A study of room-temperature $Li_xNi_{0.5}Mn_{1.5}O_4$ solid solutions. *Scientific Reports*, 5:8027 EP –, Jan 2015. Article.

[9] Bo Xu and Shirley Meng. Factors affecting li mobility in spinel $LiMn_2O_4$a first-principles study by {GGA} and gga+u methods. *Journal of Power Sources*, 195(15):4971 – 4976, 2010.

[10] Bin Hai, Alpesh K. Shukla, Hugues Duncan, and Guoying Chen. The effect of particle surface facets on the kinetic properties of limn1.5ni0.5o4 cathode materials. *J. Mater. Chem. A*, 1:759–769, 2013.

[11] Y. J. Wei, L. Y. Yan, C. Z. Wang, X. G. Xu, F. Wu, , and G. Chen*. Effects of ni doping on [mno6] octahedron in $LiMn_2O_4$. *The Journal of Physical Chemistry B*, 108(48):18547–18551, 2004.

[12] Jun Liu and Arumugam Manthiram. Understanding the improved electrochemical performances of fe-substituted 5 v spinel cathode $LiNi_{0.5}Mn_{1.5}O_4$. *The Journal of Physical Chemistry C*, 113(33):15073–15079, 2009.

[13] D. Li and Y. Xia. Electrospinning of nanofibers: Reinventing the wheel? *Advanced Materials*, 16(14):1151–1170, 2004.

[14] Heng-Guo Wang, Shuang Yuan, De-Long Ma, Xin-Bo Zhang, and Jun-Min Yan. Electrospun materials for lithium and sodium rechargeable batteries: from structure evolution to electrochemical performance. *Energy Environ. Sci.*, 8:1660–1681, 2015.

[15] Vanchiappan Aravindan, Jayaraman Sundaramurthy, Palaniswamy Suresh Kumar, Yun-Sung Lee, Seeram Ramakrishna, and Srinivasan Madhavi. Electrospun nanofibers: A prospective electroactive material for constructing high performance li-ion batteries. *Chem. Commun.*, 51:2225–2234, 2015.

[16] Ji-Won Jung, Cho-Long Lee, Sunmoon Yu, and Il-Doo Kim. Electrospun nanofibers as a platform for advanced secondary batteries: a comprehensive review. *J. Mater. Chem. A*, 4:703–750, 2016.

[17] S. Vrieze, T. Camp, A. Nelvig, B. Hagström, P. Westbroek, and K. Clerck. The effect of temperature and humidity on electrospinning. *Journal of Materials Science*, 44(5):1357–1362, 2008.

[18] Valencia Jacobs, Rajesh D. Anandjiwala, and Malik Maaza. The influence of electrospinning parameters on the structural morphology and diameter of electrospun nanofibers. *Journal of Applied Polymer Science*, 115(5):3130–3136, 2010.

[19] Wenguo Cui, Xiaohong Li, Shaobing Zhou, and Jie Weng. Investigation on process parameters of electrospinning system through orthogonal experimental design. *Journal of Applied Polymer Science*, 103(5):3105–3112, 2007.

[20] Pirjo Heikkilä and Ali Harlin. Parameter study of electrospinning of polyamide-6. *European Polymer Journal*, 44(10):3067 – 3079, 2008.

[21] C. Wang, W. Zhang, Z.H. Huang, E.Y. Yan, and Y.H. Su. Effect of concentration, voltage, takeover distance and diameter of pinhead on precursory poly (phenylene vinylene) electrospinning. *Pigment & Resin Technology*, 35(5):278–283, 2006.

[22] A. K. Haghi and M. Akbari. Trends in electrospinning of natural nanofibers. *physica status solidi (a)*, 204(6):1830–1834, 2007.

[23] Sachiko Sukigara, Milind Gandhi, Jonathan Ayutsede, Michael Micklus, and Frank Ko. Regeneration of bombyx mori silk by electrospinningpart 1: processing parameters and geometric properties. *Polymer*, 44(19):5721 – 5727, 2003. In Honour of Ian Ward's 75th Birthday.

[24] S-H. Tan, R. Inai, M. Kotaki, and S. Ramakrishna. Systematic parameter study for ultra-fine fiber fabrication via electrospinning process. *Polymer*, 46(16):6128 – 6134, 2005.

[25] Mauro R. Sardela. *X-Ray Diffraction and Reflectivity*. Springer New York, New York, NY, 2014.

[26] Jason Grebenkemper. Powder x-ray diffraction. `http://chemwiki.ucdavis.edu/Core/Analytical_Chemistry/Instrumental_Analysis/Diffraction/Powder_X-ray_Diffraction` Accessed on 23-06-2016.

[27] J. I. Langford and A. J. C. Wilson. Scherrer after sixty years: A survey and some new results in the determination of crystallite size. *Journal of Applied Crystallography*, 11(2):102–113, 1978.